JMEPEG (2010) 19:221–230
DOI: 10.1007/s11665-009-9450-6

1059-9495/$19.00

Superplastic Behavior of Al-4.5Mg-0.46Mn-0.44Sc Alloy Sheet Produced by a Conventional Rolling Process

A. Smolej, B. Skaza, and V. Dragojević

(Submitted February 6, 2009; in revised form March 12, 2009)

This article describes the superplastic behavior of the Al-4.5Mg-0.46Mn-0.44Sc alloy. The investigated alloy was produced by casting and was conventionally processed to form a sheet with a thickness of 1.9 mm and an average grain size of 11 μm. The superplastic properties of the alloy were investigated using a uniaxial tensile testing with a constant cross-head speed and with a constant strain rate in the range 1×10^{-4} to 5×10^{-2} s^{-1} at temperatures from 390 to 550 °C. The investigations included determinations of the true-stress, true-strain characteristics, the maximum elongations to failure, the strain-rate sensitivity index *m*, and the microstructure of the alloy. The *m*-values determined with the strain-rate jump test varied from 0.35 to 0.70 in the temperature interval from 390 to 550°C and strain rates up to 2×10^{-2} s^{-1}. The *m*-values decreased with increased strain during pulling. The elongations to failure were in accordance with the *m*-values. They increased with the temperature and were over 1000%, up to 1×10^{-3} s^{-1} at 480 °C and up to 1×10^{-2} s^{-1} at 550 °C. A maximum elongation of 1969% was achieved at an initial strain rate of 5×10^{-3} s^{-1} and 550 °C. The results show that the addition of about 0.4 wt.% of Sc to the standard Al-Mg-Mn alloy, fabricated by a conventional manufacturing route, including hot and cold rolling with subsequent recrystallization annealing, results in good superplastic ductility.

Keywords Al-4.5Mg-0.46Mn-0.44Sc alloy, cavitation, dynamic grain growth, elongation to failure, hardening characteristics, strain-rate sensitivity index, superplastic properties, thermomechanical treatment

1. Introduction

The 5083 (Al-Mg-Mn) alloy is one of the conventional Al alloys for superplastic forming (SPF) under special working conditions. The superplastic behavior of this alloy has been investigated extensively (Ref 1-15). These investigations have included the superplastic-related characteristics, such as the manufacturing processes of the alloy, the microstructure, the flow stresses, the maximum tensile elongations to failure, the strain-rate sensitivity indexes, the optimum working conditions for achieving these properties, the mechanisms of superplastic behavior, and models of superplastic deformation using the finite-element method (Ref 11, 14, 16). These properties were determined with commercial 5083 alloys at relatively high forming temperatures and slow or intermediate strain rates.

The requirements for achieving the superplasticity of materials are now well understood (Ref 17, 18). Recently, industrial SPF operations have required Al material that is capable of exhibiting high strain-rate superplasticity at forming rates faster than 1×10^{-2} s^{-1} and temperatures lower than 400 °C (Ref 7, 19-21). Good superplastic formability under the above-mentioned working conditions can be achieved by making a further reduction in the grain size of the material (Ref 19). There are several methods for modifying the grain sizes: (1) an appropriate thermomechanical treatment involving high reductions of material during cold rolling, (2) new forming processes, such as equal channel angular pressing (ECAP) and high-pressure torsion and accumulative roll-bonding (Ref 19, 20, 22-24), and (3) minor additions of Cu, Cr, Zr, and Sc to the base alloy (Ref 7, 12, 25-27).

It is now well established that the addition of small quantities of Sc to Al alloys such as Al-Mg leads to an increase in the superplasticity (Ref 25, 26, 28-32), although Sc is a very expensive material (Ref 33). The same reports have shown that it is possible to achieve good ductility after subjecting the Al-Mg-Sc alloy to simple processing by hot and cold rolling (Ref 28, 29). Elongations without failure of 1020% and 1130% were reported for Al-4Mg-0.5Sc (Ref 28) and for Al-6Mg-0.3Sc (Ref 29) at strain rates up to about 1×10^{-2} s^{-1} and at temperatures of 538 and 475 °C, respectively. The strain-rate sensitivity indexes were in the vicinity of $m = 0.5$. The effectiveness of Sc is a consequence of the Al_3Sc particles that stabilize the microstructure and thereby producing the superplasticity at higher strain rates in Al-Mg-Sc alloys (Ref 29).

Recently, it was established that the best way to achieve superplastic ductility in the Al-Mg-Sc alloys is by extensive grain refinement resulting from an intensive plastic strain through a process such as ECAP (Ref 25, 26, 31, 32, 34). In these studies, elongations to failure of over 2000% were achieved at strain rates and temperatures within the range normally designated as high-strain-rate superplasticity (Ref 26, 31). Currently, the main disadvantage of this process is its inability to produce large amounts of material in the form of a sheet (Ref 20).

A. Smolej and **B. Skaza**, Department of Materials & Metallurgy, University of Ljubljana, Aškerčeva 12, 1000 Ljubljana, Slovenia; and **V. Dragojević**, Impol, Aluminium Industry, Partizanska ulica 38, 2310 Slovenska Bistrica, Slovenia. Contact e-mails: anton_smolej@t-2.net and vukasin.dragojevic@impol.si.

The superplastic characteristics of the 5083 alloy have also been investigated extensively (Ref 1-15). Various slightly modified alloys have been produced on a commercial scale by hot and cold rolling. Generally, with these alloys, a maximum elongation to failure of about 400%, and rarely up to 600% (Ref 3), was achieved at relatively high temperatures within the range of 400 to 560°C and at slow or intermediate strain rates of 1×10^{-4} to 5×10^{-3} s^{-1}. The strain-rate sensitivity indexes were from 0.4 to 0.7, depending on the various thermomechanical treatments and experimental conditions. Many investigations have shown that the addition of minor amounts of Sc can enhance the plastic forming of Al-Mg-Mn alloys (Ref 27, 34, 35). A tensile elongation of 680% was reported for a conventionally manufactured Al-Mg-Mn alloy with 0.25 wt.% Sc and 0.12 wt.% Zr at 1.67×10^{-3} s^{-1} and at 490 °C (Ref 27). Modified alloys processed by ECAP are capable of elongations in range of 1000 to 2000% in the temperature interval from 250 to 500 °C and at strain rates higher than 1×10^{-2} s^{-1} (Ref 34).

This article describes the effect of a 0.44 wt.% addition of Sc on the superplastic behavior of a slightly modified commercial 5083 alloy. The examined alloy sheet was prepared using a simple thermomechanical treatment that is similar to conventional industrial processing. The aim of this investigation was to determine the optimum working conditions for achieving the best superplastic properties, which are characterized by the highest elongations to failure and the highest strain-rate sensitivity indexes. The experiments were uniaxial tensile tests at constant and variable, slow and intermediate, strain rates in the temperature range of 390 to 550 °C.

2. Experimental Procedure

The Al-4.5Mg-0.46Mn-0.44Sc alloy was prepared by induction melting using Al99.9, Mg99.8, master alloys Al-2.1Sc, Al-80Mn, and Al-5Ti-1B. The melt was cast into a steel mold with dimensions of $175 \times 80 \times 27$ mm^3. The chemical composition of the alloy is shown in Table 1.

The as-cast ingots were homogenized for 4 h at 440 °C and for 4 h at 460 °C, followed by air-cooling. The scalped ingots with a thickness of 24 mm were hot rolled at 400 °C to a thickness of 10 mm, then annealed for 4 h at 475 °C, and further cold rolled to a final sheet thickness of 1.9 mm, i.e., a total reduction of 92%. The samples for the tensile tests were machined from cold-rolled sheet along the rolling direction, with a gage section of 10 mm in length and 5.4 mm in width. The samples were annealed for 2 h at 500 °C, with the intention being to create a fully recrystallized microstructure.

The uniaxial tests on the investigated alloy were carried out using a Zwick Z250 universal testing machine with a 0.5 kN load cell. The machine was equipped with a three-zone electrical resistance furnace that maintained the test temperature with an accuracy of ±2 °C. The testing chamber with the controlled temperature was over 300 mm in length. The testing procedure and the evaluation of the results were controlled by the PO software system Texespert II.

Table 1 The chemical composition of the investigated alloy (in wt.%)

Si	Fe	Mn	Mg	Ti	B	Sc	Al
0.0064	0.0018	0.466	4.55	0.0213	0.0016	0.435	Bal.

The specimens were annealed for 30 min prior to testing to ensure a uniform and stable temperature in the furnace. The measurements included determinations of the flow stresses as a function of the true strains, the elongations to failure, and the strain-rate sensitivity indexes. The testing temperatures and strain rates ranged from 390 to 550 °C and from 1×10^{-4} to 5×10^{-2} s^{-1}, respectively. The tensile tests were conducted at constant strain rates (CSR) with a continuous change of the cross-head speed and with constant cross-head speed (CCHS), where the initial strain rate decreased with the increasing strain. The strain-rate sensitivity indexes were determined using the "jump test" method. The microstructure of the untested and tested samples, like the cavitation, was examined using light microscopy.

3. The Effect of Strain Rate and Temperature on the Flow Stress

The superplastic behavior of the material is characterized by the true stress' dependence on the true strain. The true-stress, true-strain curves were determined during a CSR tensile test and during a CCHS tensile test at various temperatures and strain rates. Figure 1 shows the set of stress-strain curves at temperatures in the range from 390 to 550 °C at an initial strain rate (CCHS) of 7.5×10^{-4} s^{-1}. The shapes of the curves change with the temperatures. In all cases, there is an immediate hardening followed by a strain softening at lower temperatures and a slightly increased hardening at higher temperatures (>480 °C). This increased hardening is reduced, or even disappears, at higher initial strain rates over 1×10^{-2} s^{-1} (Fig. 2).

The hardening characteristics of the pulled specimens during the CCHS test depend on the test conditions (Fig. 3). At a temperature of 550 °C, the flow stresses increase with the strain to an initial strain rate of approximately 1×10^{-2} s^{-1}, whereas in the case of 480 °C, the plots show a consistent softening of the specimens with increased strain for all CCHS.

The tests were also conducted with a CSR. The true-stress, true-strain curves for the specimens at a CSR and at 550 °C are shown in Fig. 4. All the curves have similar shapes. The flow

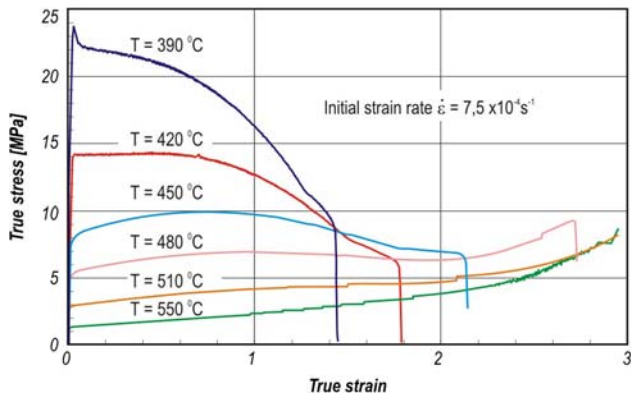

Fig. 1 True-stress, true-strain curves for various tested temperatures at an initial strain rate of 7.5×10^{-4} s^{-1} (CCHS)

stresses explicitly depend on the strain rate; they increase at higher rates. After a rapid jump in the stresses on loading, the hardening increases to a peak stress, followed by a gradual softening to failure. The peak stresses are shifted toward lower strains at higher strain rates.

The stress-strain characteristics differ depending on the test used. Figure 5 compares the true-stress, true-strain curves obtained during CSR and CCHS tests for two different constant and initial strain rates at 550 °C. The CCHS exhibits a lower strain hardening than the corresponding CSR tests.

4. Elongation

The elongation to failure is often used as an appropriate measure for the superplastic behavior of a material because, in addition to the chemical composition, it depends on the working conditions, such as the temperature and the strain rate. The elongations were measured with a tensile test under a CSR and under a CCHS at temperatures ranging from 390 to 550 °C and at strain rates (CSR and CCHS) from 1×10^{-4} to 5×10^{-2} s^{-1}. The elongation depends a great deal on the test temperature (Fig. 6, 7) and on the strain rate (Fig. 8, 9). The occurrence of true superplasticity in the alloy is demonstrated in Fig. 7, where the samples are shown after pulling to failure at various temperatures and at an equal initial strain rate of 7.5×10^{-4} s^{-1}. There is no necking in the samples, even at lower temperatures.

Elongations to failure of over 1000% were achieved at initial strain rates up to 1×10^{-3} s^{-1} and 480 °C (the maximum elongation was 1426% at 7.5×10^{-4} s^{-1}), up to 2.5×10^{-3} s^{-1} and 510 °C (the maximal elongation was 1870% at 7.5×10^{-4} s^{-1}), and up to 1×10^{-2} s^{-1} and 550 °C (the maximum elongation was 1969% at 5×10^{-3} s^{-1}). Elongations from

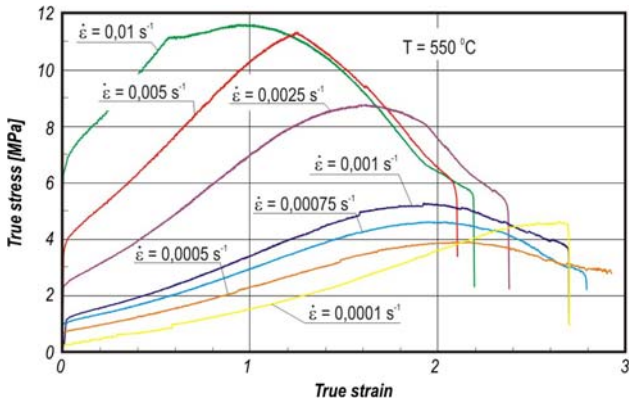

Fig. 4 True-stress, true-strain curves for various constant strain rates at 550 °C

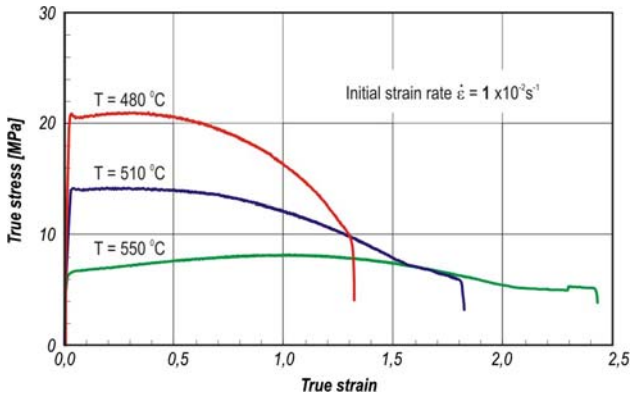

Fig. 2 True-stress, true-strain curves for three tested temperatures at an initial strain rate of 1×10^{-2} s^{-1} (CCHS)

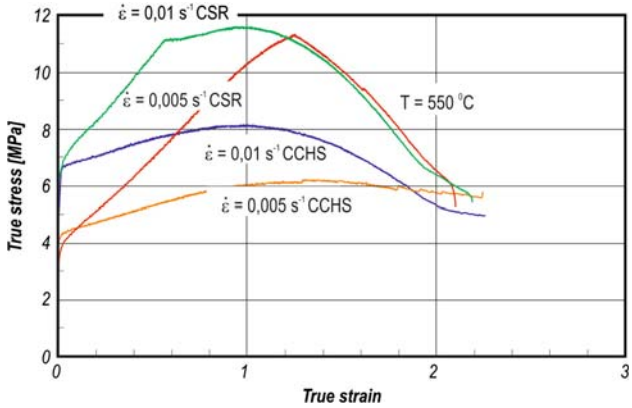

Fig. 5 Comparison of the stress-strain curves obtained during CSR and CCHS tests at 550 °C

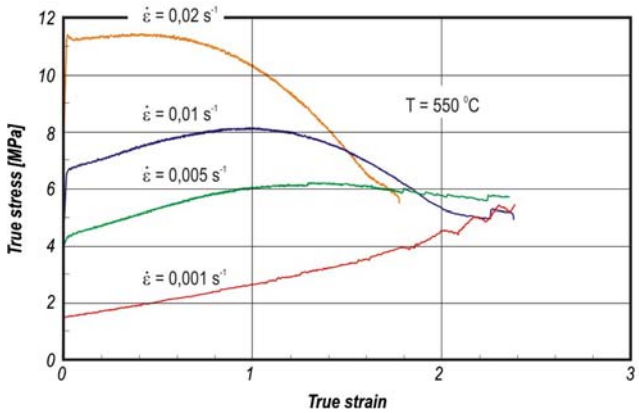

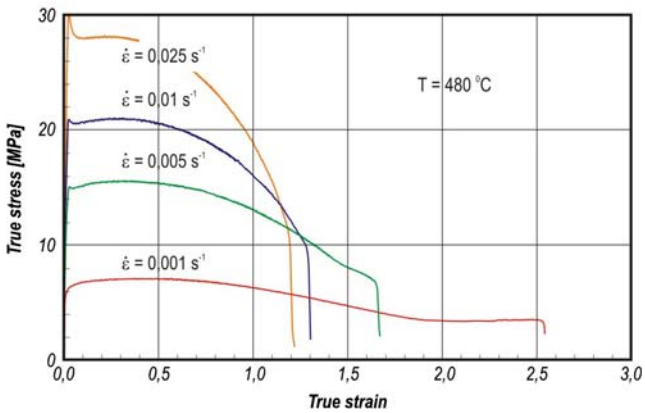

Fig. 3 True-stress, true-strain curves for various initial strain rates at 550 °C (left) and 480 °C (right)

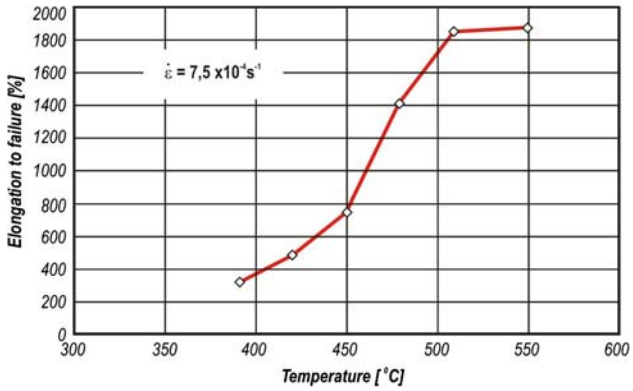

Fig. 6 Elongation to failure as a function of the test temperature at an initial strain rate of 7.5×10^{-4} s^{-1} (CCHS)

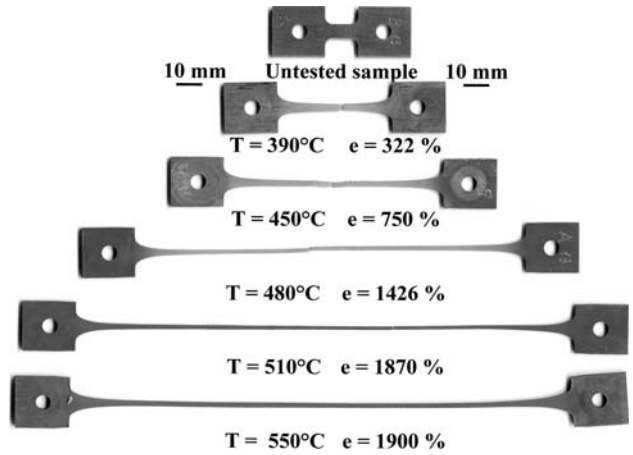

Fig. 7 Examples of superplasticity in samples after tensile testing at various temperatures at an initial strain rate of 7.5×10^{-4} s^{-1} (CCHS)

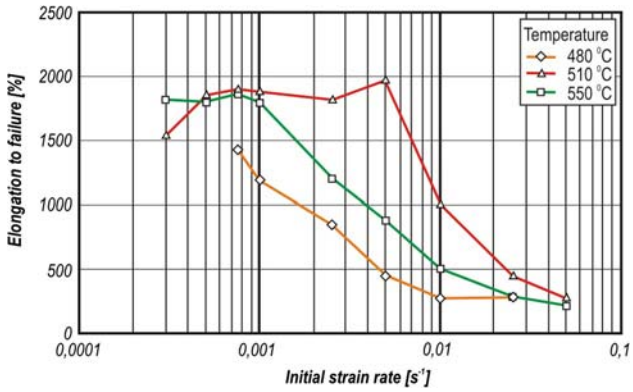

Fig. 8 Elongation to failure as a function of the initial strain rate at three temperatures

220 to 510% were obtained in the temperature interval from 480 to 510 °C in the range of higher initial strain rates from 2.5×10^{-2} to 5×10^{-2} s^{-1} (Fig. 8). Figure 9 shows the true superplasticity of samples at 550 °C and at various initial strain rates (CCHS), where the upper sample is untested. The samples show a uniform deformation within the gage length without any

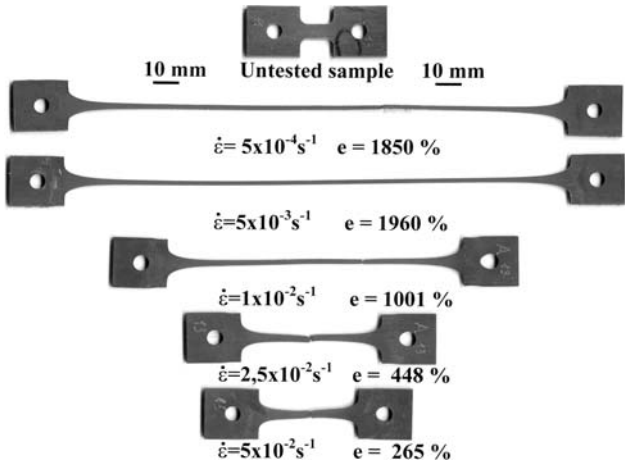

Fig. 9 Samples after tensile testing to failure at different initial strain rates at 550 °C

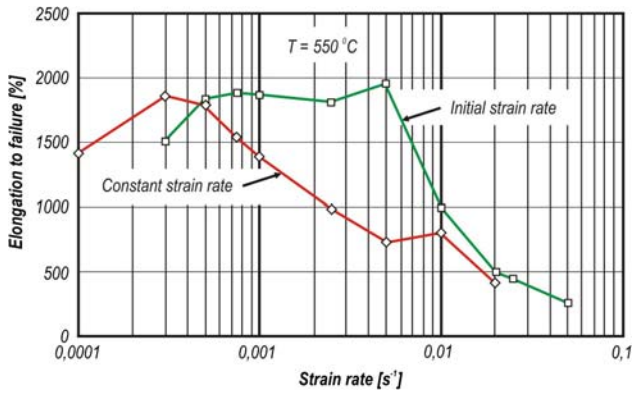

Fig. 10 A comparison of elongations to failure as a function of constant strain rate (CSR test) and of initial strain rate (CCHS test) at 550 °C

necking to failure. Since a 200% elongation can be considered as an initial indicator of superplasticity, elongations at higher strain rates over 1×10^{-2} s^{-1} (CCHS test) are still in the area of the superplastic regime at all the tested temperatures.

The elongation values achieved during tensile tests with a CSR and a CCHS (both tests starting at the same initial strain rate) are not equal at the same testing temperature, which is shown in Fig. 10. The elongation peak of the samples during the CSR test is displaced to slower strain rates in comparison to the CCHS test. The elongations to failure of the CSR test are generally lower and decrease with an increased strain rate after the peak elongation. The CCHS test makes it possible to achieve total elongations in excess of 1500% across a wider range of intermediate strain rates, from 5×10^{-4} to 5×10^{-3} s^{-1} at 550 °C and from 5×10^{-4} to 1×10^{-3} s^{-1} at 510 °C.

5. The Strain-Rate Sensitivity Index *m* of the Tested Alloy

The strain-rate sensitivity index m is one of the most important parameter that characterizes superplastic deformation. Higher m-values indicate an increased resistance to

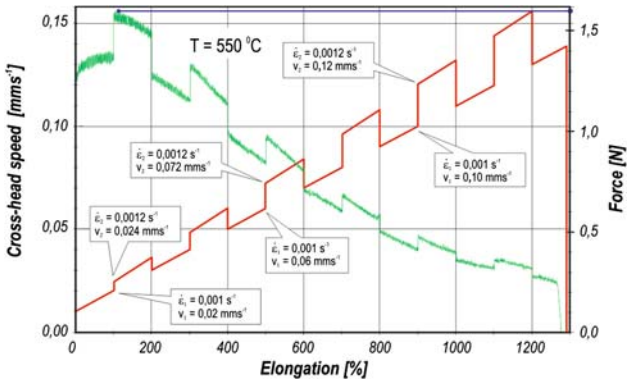

Fig. 11 The change of cross-head speed during the multi-strain-rate jump test

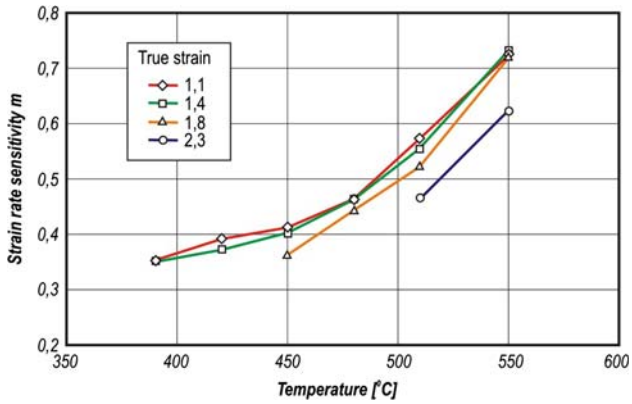

Fig. 12 The strain-rate sensitivity index m as a function of the test temperature for various strains (the strain-rate jump test at downward $\dot{\varepsilon}_1 = 3 \times 10^{-4}$ s^{-1} and upward $\dot{\varepsilon}_2 = 8 \times 10^{-4}$ s^{-1})

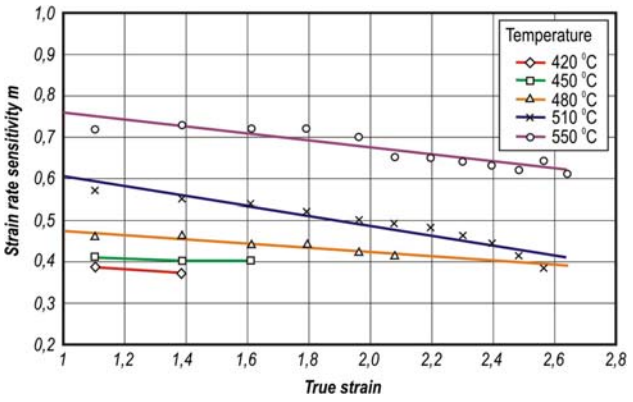

Fig. 13 The strain-rate sensitivity index m as a function of the true strain for various tested temperatures at a constant downward strain rate $\dot{\varepsilon}_1 = 3 \times 10^{-4}$ s^{-1}

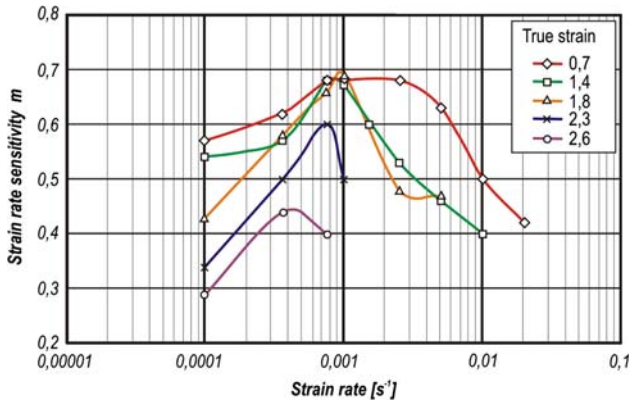

Fig. 14 The strain-rate sensitivity index m as a function of strain rate for various strains at 550 °C (the jump test with a 20% increase of the strain rates)

necking, and thus they allow large elongations to failure. There are several experimental methods to determine the m-value (Ref 18, 36). In this study, the m-values as a function of the strain rate and the test temperature were estimated using the multi-strain-rate jump test. This test to determine the m-values as a function of strain rate over the range from 1×10^{-4} to 2×10^{-2} s^{-1} was conducted by increasing and decreasing the strain rate by 20% at every increment of 100% elongation. The strain rates were constant during the single jumps that were controlled by the software for a continuous change of cross-head speed. In Fig. 11, the change of cross-head speed is shown as an example of increasing the strain rate from $\dot{\varepsilon}_1 = 1 \times 10^{-3}$ s^{-1} (downward strain rate) up to $\dot{\varepsilon}_2 = 1.2 \times 10^{-3}$ s^{-1} (upward strain rate) during progressive elongation, and the corresponding simultaneous change of force. The m-values were calculated using the equation:

$$m = \frac{\log \frac{\sigma_2}{\sigma_1}}{\log \frac{\dot{\varepsilon}_2}{\dot{\varepsilon}_1}} = \frac{\log \frac{F_2}{F_1}}{\log \frac{v_2}{v_1}}$$

where σ_1, σ_2 are the stresses, $\dot{\varepsilon}_1, \dot{\varepsilon}_2$ are the corresponding instantaneous strain rates, F_1, F_2 are the forces, and v_1, v_2, are the cross-head speeds before and after the jump. By convention, the m-value is attributed to the downward strain rate $\dot{\varepsilon}_1$ (Ref 18). The multi-strain-rate jump makes possible the examination of the m-values at various progressive strains or elongations at a fixed strain rate during a single test. Similarly, the m-values were also determined as a function of the test temperature, where the downward constant strain rate was 3×10^{-4} s^{-1} and the upward value was 8×10^{-4} s^{-1}.

The m-value as a function of testing temperature at 390, 430, 450, 480, 510, and 550 °C to four true-strain levels is shown in Fig. 12. For all the strains, the m-value increases with the temperature. The maximum value of 0.7 occurs at 550 °C, and the lowest value of 0.35 occurs at 390 °C, which still ensures the superplastic forming. In the temperature range between 420 and 480 °C, the m-value varies from 0.4 to 0.45. These data relate to a true strain of 1.1 (200%). The index m changes at a single temperature with the increasing strain (Fig. 13).

The indexes m, calculated from the jump tests, are plotted as a function of the strain rate for strains over the range from 0.7 (100%) to 2.6 (1300%) at the test temperature, 550 °C, in Fig. 14. The index m is changed at all strains with the strain rates; the data demonstrate the bell-shaped curvature that is typical of superplastic materials. The m-value increases from the lowest strain rate of 1×10^{-4} s^{-1}. The m plots show peaks that occur within a narrow range of strain rates, from 3.6×10^{-4} to 1×10^{-3} s^{-1}. A maximum value of $m = 0.68$ was obtained in this range at a true strain of $\varepsilon = 0.7$ and $m = 0.44$ at $\varepsilon = 2.6$ and at a strain rate of 3.6×10^{-4} s^{-1}.

The peaks of the m plots are shifted to lower strain rates at higher strains. The m-values at strain rates above 5×10^{-3} s^{-1} are still of an order of magnitude that is required for superplastic materials, which is important from the technical point of view. The m-values are consistent with the data shown in Fig. 8, i.e., the high m-values result in a high tensile elongation without necking. Figure 15 shows the m-change with increased strain in a similar way to Fig. 14. The smallest change is in the range of the highest m-values, at strain rates between 7.5×10^{-4} and 1×10^{-3} s^{-1}.

6. Microstructure and Cavitation

The microstructure of the alloy was examined with respect to the grains under the conditions of static annealing in the grip section and during superplastic forming in the gage section of the samples at an initial strain rate of 7.5×10^{-4} s^{-1} and 550 °C. The starting microstructure consisted of recrystallized, equiaxed grains caused by isothermal annealing for 2 h at 500 °C prior to the tensile test. The average initial grain size was about 11 μm. Optical micrographs of the grains from the gage section of the samples that were strained to various elongations are presented in Fig. 16.

The dynamic and static grain growth as a function of annealing time during the tensile test is shown in Fig. 17. The static grain growth, measured in the grip region of the longitudinal section, increases at the beginning of the annealing, after which the grains were stable. The dynamic grain growth is approximately two times higher than the static growth for all elongations in the interval from 200 to 1900%. The average grain size at higher elongations is about three times greater than the starting size before the superplastic forming. This is consistent with the notion that a longer forming time results in a longer exposure to temperature, which results in more grain growth (Ref 8). The duration of the dynamic grain growth, for example, at an initial strain rate of 7.5×10^{-4} s^{-1}, was about 45 min for 200% and about 420 min for 1900%. The grains in the gage section were slightly elongated, with an aspect ratio of about 1.6, which remained nearly constant for all elongations.

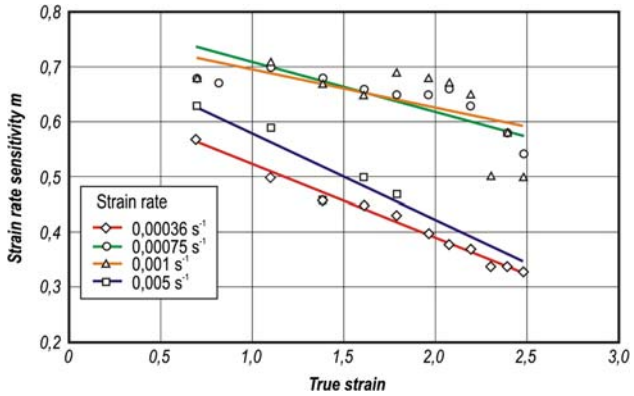

Fig. 15 The dependence of the strain-rate sensitivity index m on the true strain for various strain rates at 550 °C

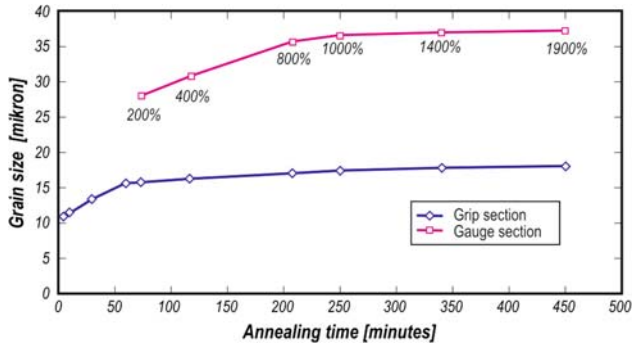

Fig. 17 Static and dynamic grain growth measured in the longitudinal grip and the gage section of samples at 550 °C and at an initial strain rate of 7.5×10^{-4} s^{-1}

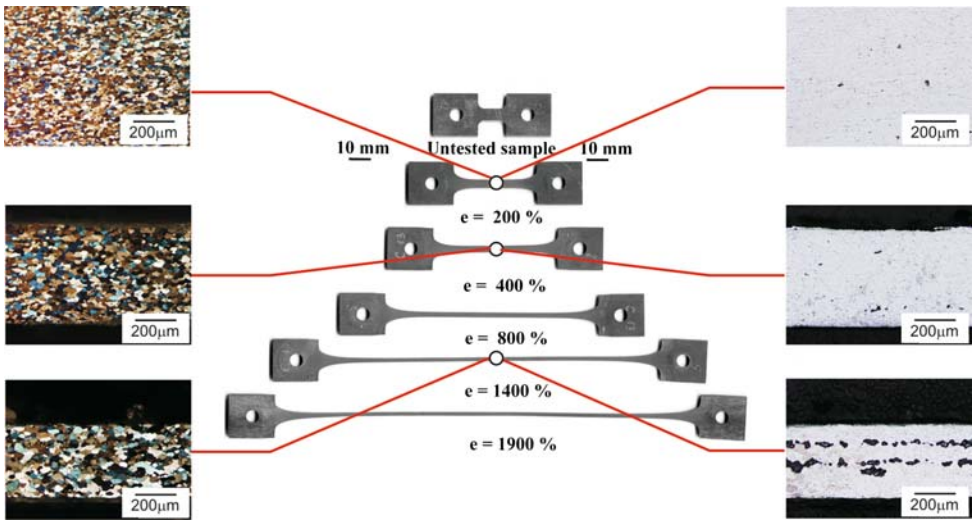

Fig. 16 Samples after tensile testing at various elongations with microstructures and cavitations in the gage length at 550 °C and an initial strain rate of 7.5×10^{-4} s^{-1}

The cavitation of the alloy during the superplastic forming was examined with the same samples and under the testing conditions described in Fig. 16. The fraction of cavitation was determined by measuring the cavity area on the surface in the longitudinal and transverse sections of the samples (Fig. 18).

The percentage of cavitation increases with the increasing strain, in a similar way for all the measured areas. The cavities are randomly distributed within the volume of the specimens up to 800% of elongation. At higher elongations, the cavities form stringers in the tensile direction (Fig. 16). These stringers are more clearly observed above 1400%. The greatest cavitation occurs in the middle of the longitudinal section, and the occurrence of cavities influences the failure mechanism. Figure 19 shows the fracture surface of a sample deformed to 289% at 2.5×10^{-2} s^{-1}. The fracture is mainly intergranular, with only a few dimples. The fractures of samples pulled to 1819% at a slower initial rate of 3×10^{-4} s^{-1} show large cavities as a consequence of the coalescence of smaller voids. The internal cavitation has a greater role in the failure mechanism, particularly at slower strain rates, in comparison to the microstructural evolution during superplastic forming.

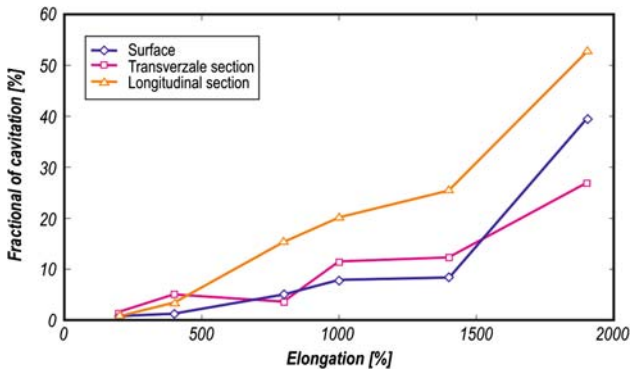

Fig. 18 Fraction of cavitation in the gage length of the pulled samples as a function of the elongation after the tensile test at 550 °C and 7.5×10^{-4} s^{-1}. The percentage of cavitation was measured on the surface both in the transverse section and the longitudinal section of the samples

7. Discussion

The investigated Al-4.5Mg-0.46Mn-0.44Sc alloy is a modification of the commercial 5083 alloy. It is known that additions of Sc to Al alloys act as a grain refiner during the casting and stabilize the grain structure from Al_3Sc dispersoids, which are essential characteristics for good superplasticity (Ref 28, 29, 33). The addition of Sc to Al-Mg-Mn alloys results in a uniform distribution of fine coherent Al_3Sc precipitates which effectively pinned the grain boundaries during the recrystallization (Ref 29). Compared with other grain-refining elements used in Al alloys, e.g., Ti and Zr, more Sc must be added for effective refinement. The addition of 0.44 wt.% Sc in the investigated alloy is in excess of the maximum solid solubility of Sc in the Al matrix, which is approximately 0.38 wt.% (Ref 29, 33). A nominal quantity of 0.45 wt.% Sc in the investigated alloy was chosen on the basis of preliminary experiments with the Al-4.5Mg-Sc alloy, containing Sc in the range of 0.1 to 0.5 wt.%. The finest microstructure, with an average grain size of about 40 μm in the as-cast state, was obtained in the alloy with the greatest Sc content.

The strain-hardening characteristics during the superplastic deformation of the investigated alloy depend on the test temperature, the strain rate, and the method of testing. After a rapid jump of the stresses on loading, the flow stresses under CSR tests further increase with increased strain up to a stress maximum, followed by a softening to failure (Fig. 4). The slopes of the stress-strain curves decrease during the hardening process with decreased CSR and the peak stresses are pushed toward higher strains. These differences in hardening behavior can be explained by the deformation mechanisms operating during the pulling of the samples (Ref 2, 3). In theory, the process of grain-boundary sliding and dislocation slip can control the superplastic deformation (Ref 2, 3, 8, 27, 29). The deformation mechanism of the samples tested at a lower CSR ($<1 \times 10^{-3}$ s^{-1}) is most likely to be grain-boundary sliding. The hardening at a lower CSR is probably the cause of the dynamic grain growth. As the grains grow, the required stress to continue deformation increases (Ref 8). At higher strain rates ($>1 \times 10^{-3}$ s^{-1}), the hardening is a result of dislocation

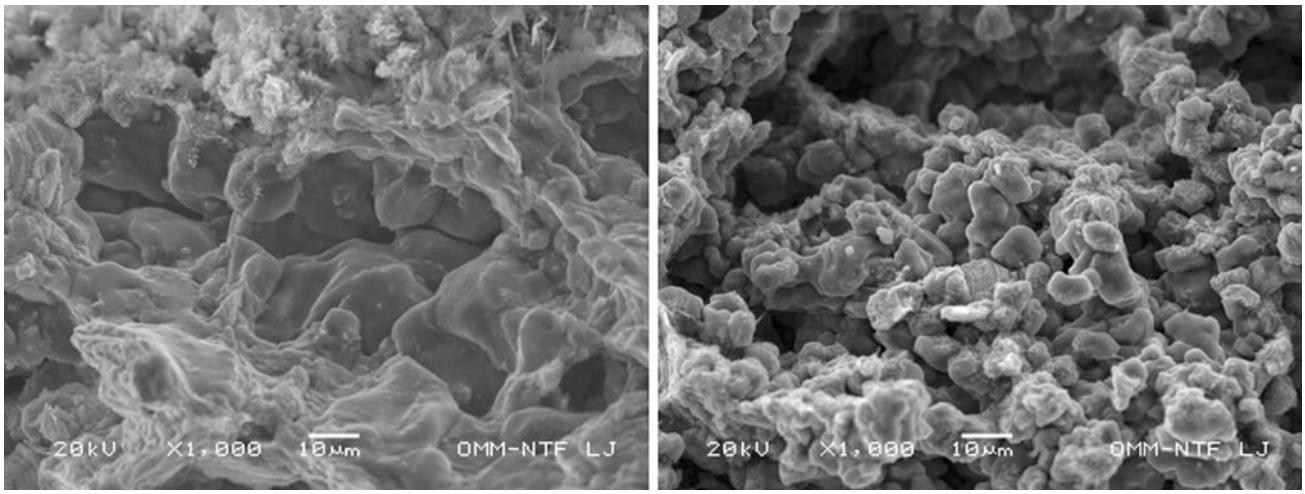

Fig. 19 SEI images of the fracture surface of the tested specimens at 510 °C: at an initial strain rate of 3×10^{-4} s^{-1} (left, e = 1819%) and of 2×10^{-2} s^{-1} (right, e = 289%)

multiplication and of the interaction between the dislocations and the fine particles in the matrix.

The tests were also conducted at a CCHS. The shapes of the true-stress, true-strain curves depend on the working temperatures and the initial strain rates (Fig. 1-3). After a rapid increase of the stresses to approximately 5% strain, the tests performed at faster initial strain rates show no, or very little, increase in the flow stresses, whereas there is an appearance of hardening during the slower CCHS tests. The reason for the strain hardening of the material, especially at higher temperatures (>480 °C) and lower initial strain rates ($<1 \times 10^{-2}$ s^{-1}), is the grain growth (Ref 29, 34). The samples pulled at a lower CCHS are exposed for longer times to relatively high temperatures, which enhances the process of grain growth.

The CSR tests cause higher flow stresses, higher strain hardening, and lower strains to failure in comparison to the CCHS tests, if both tests start at the same initial strain rate (Fig. 5). This is to be expected because when the specimens are forming during the CCHS test the strain rate continuously decreases, which promotes the process of grain-boundary sliding. The initial strain rate, for example, of 7.5×10^{-4} s^{-1} during the CCHS test is reduced to 4×10^{-4} s^{-1} at a strain of $\varepsilon = 1.1$ (~200%). For all the examined conditions, steady-state flow did not appear. Generally, the shapes of true-stress, true-strain curves of the investigated Al-4.5Mg-0.46Mn-0.44Sc alloy are comparable to the curves of alloys with a similar composition, like Al-Mg-Mn (Ref 2, 3, 8), Al-Mg-Sc (Ref 29, 34), and Al-Mg-Mn-Sc (Ref 27). However, there are certainly some differences in the flow stresses and the strains to failure because of the different compositions of the alloys and the testing conditions.

The elongations to failure depend on the strain rate and the test temperature. The total elongations achieved with the CCHS tests increase with a decreasing initial strain rate up to a peak maximum. There is also a large increase of the elongations with an increased temperature, especially in the range of 450 to 550 °C at intermediate strain rates from 7.5×10^{-4} to 1×10^{-2} s^{-1} (Fig. 6, 8). The different tensile elongations achieved with the CCHS and CSR tests under the corresponding test conditions (temperature, equal initial, and constant strain rate) are the consequence of a continuously decreasing strain rate during the CCHS test, which results in larger elongations.

The investigated alloy was prepared from high-purity Al. It is known that the increased iron content reduces formability of these alloy types. The iron combines with other alloying elements, the particles that act as nucleation sides for cavitations during the deformation (Ref 13). It has been reported that the maximal elongations to failure of 5083 alloys made from high-purity Al (SKY5083) are at similar deformation conditions like in this work in the range of about 300 to 600% (Ref 3, 9, 13, 37, 38). These elongations are much lower than the alloys with Sc.

The strain-rate sensitivity index m varies with the test temperature, the strain rate, and the strain. The variation of the m-value is similar to that of the elongation to failure: high elongations are associated with high m-values. The m-value, determined by a jump test at a CSR, increases with the increasing test temperature (Fig. 12) and varies with the strain rate (Fig. 14). The highest m-values in the range of 0.50 to 0.68 occur at 550 °C, within the interval of constant strain rates, from 3.6×10^{-4} to 1×10^{-3} s^{-1}, at strains lower than $\varepsilon < 2.3$ (900%). The m-values decrease on both sides of the peak maximum, with decreasing and increasing strain rates. The m-values determined at lower strains $\varepsilon < 1.8$ (500%) and at a temperature of 550 °C exceed the value of 0.4 in the range of the strain rates from 1×10^{-4} to 1×10^{-2} s^{-1}. The m-values at CSR and constant temperature decrease with the increased strain (Fig. 13, 15), which is more pronounced at higher temperatures and slower (3.6×10^{-4} s^{-1}) or higher (5×10^{-3} s^{-1}) constant strain rates. The decrease of the m-values is most likely due to the consequence of a combination of the grain-growth process and the progressive cavitation (Ref 8). The reason for the variation of m-values as a function of the strain rate is, apart from the grain growth and the cavitation, also connected with the mechanism of superplastic deformation. At relatively slow and intermediate strain rates, where the m-values and the elongations to failure at higher temperatures are the highest, the main mechanism of superplastic forming is grain-boundary sliding, accommodated by grain-boundary diffusion. At relatively high strain rates, the deformation of the alloy is controlled by thermally assisted dislocation motion (Ref 8).

The starting microstructure of the samples prior to a tensile test consisted of fully recrystallized grains with an average grain size of 11 μm. Such a grain size is still considered to be fine for Al alloys from the superplasticity point of view. During the subsequent annealing and pulling of the samples, static and dynamic grain growth occurred. The grain size in the grip and gage sections changed very little after a certain time of annealing (approximately 60 min) and elongation (approximately 800%) under the forming conditions at 550 °C and 7.5×10^{-4} s^{-1}. In this region, the aspect ratio remains nearly constant at about 1.6. The value of the aspect ratio is typical for superplastic alloys where there is a large contribution of grain-boundary sliding in the total elongation (Ref 34). The grain size in the gage length at larger elongations is up to three times larger in comparison to the initial size, which is unusual for superplastic Al alloys. The intensive, dynamic grain growth tends to deteriorate the superplastic deformation because of the increasing flow stresses and cavitation, which nucleates preferentially at the grain boundaries (Ref 3). Despite the relatively larger grains, very large elongations, up to 2000%, were achieved with this alloy.

The failure of these types of alloys is often the result of internal cavitation (Ref 8). Extensive cavitation, which in addition to larger grains, is a limiting factor for superplasticity, appeared at over 800%. The percentage of cavitation in this range increased from about 15 to 50% at an elongation of 1900%, whereas the grains in the longitudinal gage section grew only from 35 to 37 μm at a constant aspect ratio. Despite the larger grains, elongations up to 2000% were achieved, which depends first of all on high values of the strain-rate sensitivity index and on the resistance to necking. In this alloy, the cavitation predominates over the grain size as the reason for the premature failure of the specimens during tensile deformation. This suggests that it is possible with this alloy to achieve a further increase in the elongation with a simultaneous decrease in the amount of cavitation. It is well known that elongations in range of 300 to 400% are most often required for industrial superplastic forming (Ref 21, 39). It is possible to achieve this requirement with a relatively simple thermomechanical treatment of the alloy and with sheet forming above 390 °C at medium initial or constant strain rates in the range of 5×10^{-4} to 2×10^{-2} s^{-1}.

The investigated Al-4.5Mg-0.46Mn-0.44Sc alloy with a recrystallized grain size of about 11 μm, which was produced by a simple thermomechanical treatment, showed good superplastic ductility in the temperature interval from 390 to 550 °C and at intermediate strain rates up to 2×10^{-2} s^{-1}. There are a lot of earlier reports on superplasticity for standard Al-Mg-Mn (5083) alloys that were thermomechanically processed (Ref 2, 3, 5, 6, 8, 9, 12, 13). This alloy, without any Sc addition, exhibited elongations to failure, mostly up to 600%, with *m*-values in the range of 0.4 to 0.65 at strain rates from 1×10^{-4} to 1×10^{-2} s^{-1} and at temperatures of 450 to 550 °C. The addition of about 0.4 wt.% of Sc to the 5083 alloy makes it possible to obtain greater elongations to failure by a factor of about three for similar testing conditions.

8. Summary and Conclusions

1. The Al-4.5Mg-0.46Mn-0.44Sc alloy was produced by ingot casting and by a simple thermomechanical rolling process. The sheet, 1.9 mm thick, with an average grain size of 11 μm, was the starting material for the superplastic deformation.
2. The true-stress, true-strain characteristics of the investigated alloy differ with respect to the test conditions and to the type of test used. The CCHS test results in less strain hardening of the alloy than the corresponding CSR test.
3. The elongation to failure increases with higher temperatures. The elongations of the tests conducted at temperatures above 480 °C exceeded 1000% at initial strain rates up to 1×10^{-3} s^{-1}; above 510 °C, they were up to 2.5×10^{-3} s^{-1}, and at 550 °C, they were up to 1×10^{-2} s^{-1}. A maximum elongation of 1969% was achieved at an initial strain rate of 5×10^{-3} s^{-1}.
4. While a 200% elongation can be considered as an initial indicator of superplasticity, elongations of this alloy at higher strain rates $> 1 \times 10^{-2}$ s^{-1} (CCHS) are still in the area of the superplastic regime at test temperatures in the range of 480 to 550 °C.
5. The CCHS tests show larger tensile elongations than the CSR tests (both tests starting at the same initial strain rate). The CCHS tests make it possible to achieve total elongations in excess of 1500% across a wider range of intermediate initial strain rates between 5×10^{-4} and 5×10^{-3} s^{-1} at 550 °C and up to 1×10^{-3} s^{-1} at 510 °C.
6. The *m*-values of the CSR test in the temperature range of 390 to 550 °C and at 3×10^{-4} s^{-1} are 0.35 to 0.70. The *m*-value varies with the strain rate and has its highest values from 0.50 to 0.68 at strain rates between 3.6×10^{-4} and 1×10^{-3} s^{-1}, measured at 550 °C for strains lower than $\varepsilon < 2.3$ (900%). The *m*-value decreases with the increased strain during pulling under constant test conditions.
7. The dynamic grain growth of the alloy during superplastic deformation is approximately twice as high as the static grain growth at elongations ranging from 200 to 1900% at 550 °C. The average grain size at higher elongations is about three times greater than the starting size before the superplastic forming.
8. The percentage of cavitation increases with the increasing strain; it is about 15% at 800% elongation and about 53% at 1900%.
9. The addition of about 0.4 wt.% of Sc to a standard Al-Mg-Mn (5083) alloy produced by a simple thermomechanical treatment, including hot and cold rolling with subsequent recrystallization annealing, results in good superplastic ductility, which is reflected in large elongations in the temperature interval from 390 to 550 °C and at strain rates up to 2×10^{-2} s^{-1}.

Acknowledgment

This work was supported by Slovenian Research Agency (ARRS), Government of the Republic of Slovenia.

References

1. J.S. Vetrano, C.A. Lavender, C.H. Hamilton, M.T. Smith, and S.M. Bruemmer, Superplastic Behaviour in a Commercial 5083 Aluminium Alloy, *Scr. Metall. Mater.*, 1994, **30**, p 565–570
2. R. Verma, A.K. Ghosh, S. Kim, and C. Kim, Grain Refinement and Superplasticity in 5083 Al, *Mater. Sci. Eng. A*, 1995, **191**, p 143–150
3. R. Verma, P.A. Friedman, A.K. Ghosh, S. Kim, and C. Kim, Characterization of Superplastic Deformation Behaviour of a Fine Grain 5083 Al Sheet, *Metall. Mater. Trans. A*, 1996, **27**, p 1889–1898
4. F. Li, W.T. Roberts, and P.S. Bate, Superplasticity and the Development of Dislocation Structures in an Al-4.5%Mg Alloy, *Acta Mater.*, 1996, **44**(1), p 217–233
5. H. Iwasaki, H. Hosokawa, T. Mori, T. Tagata, and K. Higashi, Quantitative Assessment of Superplastic Deformation Behavior in a Commercial 5083 Alloy, *Mater. Sci. Eng. A*, 1998, **252**, p 199–202
6. I.C. Hsiao and J.C. Huang, Development of Low Temperature Superplasticity in Commercial 5083 Al-Mg Alloys, *Scr. Mater.*, 1999, **40**(6), p 697–703
7. I.C. Hsiao, J.C. Huang, and S.W. Su, Grain Structure, Texture Evolution and Deformation Mechanism During Low Temperature Superplasticity in 5083 Al-Mg Alloy, *Mater. Trans. JIM*, 1999, **40**(8), p 744–753
8. P.A. Friedman and W.B. Copple, Superplastic Response in Al-Mg Sheet Alloys, *J. Mater. Eng. Perform.*, 2004, **13**(3), p 335–347
9. R.M. Cleveland, A.K. Ghosh, and J.R. Bradley, Comparison of Superplastic Behavior in Two 5083 Aluminium Alloys, *Mater. Sci. Eng. A*, 2003, **351**, p 228–236
10. L.D. Hefti, Commercial Airplane Applications of Superplastically Formed AA5083 Aluminium Sheet, *J. Mater. Eng. Perform.*, 2007, **16**(2), p 136–141
11. S. Agarwal, C.L. Briant, P.E. Krajewski, A.F. Bower, and E.M. Taleff, Experimental Validation of Two-dimensional Finite Element Method for Simulating Constitutive Response of Polycrystals During High Temperature Plastic Deformation, *J. Mater. Eng. Perform.*, 2007, **16**(2), p 170–178
12. R. Verma and S. Kim, Superplastic Behavior of Copper-Modified 5083 Aluminium Alloy, *J. Mater. Eng. Perform.*, 2007, **16**(2), p 185–191
13. Y. Luo, C. Miller, G. Luckey, P. Friedman, and Y. Peng, On Practical Forming Limits in Superplastic Forming of Aluminium Sheet, *J. Mater. Eng. Perform.*, 2007, **16**(3), p 274–283
14. H. Raman, G. Luckey, G. Kridli, and P. Friedman, Development of Accurate Constitutive Models for Simulation of Superplastic Forming, *J. Mater. Eng. Perform.*, 2007, **16**(3), p 284–292
15. M.A. Kulas, P.E. Krajewski, J.R. Bradley, and E.M. Taleff, Forming-Limit Diagrams for Hot-Forming of AA5083 Aluminium Sheet: Continuously Cast Material, *J. Mater. Eng. Perform.*, 2007, **16**(3), p 308–313
16. N. Chandra, S.C. Rama, and Z. Chen, Critical Issues in the Industrial Application of SPF-Process Modeling and Design Practices, *Mater. Trans. JIM*, 1999, **40**(8), p 723–736
17. T.G. Langdon, The Mechanical Properties of Superplastic Materials, *Metall. Trans. A*, 1982, **13**(5), p 689–701
18. K.A. Padmanabhan, R.A. Vasin, and F.U. Enikeev, Phenomenology of Superplastic Flow, *Superplastic Flow: Phenomenology and Mechanics*, Springer Verlag, Berlin Heidelberg, New York, 2001, p 5–26

19. T.G. Langdon, Recent Developments in High Strain Rate Superplasticity, *Mater. Trans. JIM*, 1999, **40**(8), p 716–722
20. N. Tsuji, K. Shiotsuki, and Y. Saito, Superplasticity of Ultra-Fine Grained Al-Mg Alloy Produced by Accumulative Roll-Bonding, *Metall. Trans. JIM*, 1999, **40**(8), p 765–771
21. K. Higashi, High Strain Rate Superplasticity in Japan, *Mater. Sci. Technol.*, 2000, **16**, p 1320–1329
22. M. Kawasaki, R.B. Figueiredo, C. Xu, and T.G. Langdon, Developing Superplastic Ductilities in Ultrafine-Grained Metals, *Metall. Mater. Trans. A*, 2007, **38**(9), p 1891–1898
23. Z. Horita, M. Furukawa, N. Nemoto, and T.G. Langdon, Development of Fine Grained Structures Using Severe Plastic Deformation, *Mater. Sci. Technol.*, 2000, **16**, p 1239–1245
24. T.G. Langdon, The Processing of Ultrafine-Grained Materials Through the Application of Severe Plastic Deformation, *J. Mater. Sci.*, 2007, **42**(10), p 3388–3397
25. P.B. Berbon, S. Komura, A. Utsunomiya, Z. Horita, M. Furukawa, M. Nemoto, and T.G. Langdon, An Evaluation of Superplasticity in Aluminium-Scandium Alloys Processed by Equal-Channel Angular Pressing, *Mater. Trans. JIM*, 1999, **40**(8), p 772–778
26. M. Furukawa, A. Utsunomiya, K. Matsubara, Z. Horita, and T.G. Langdon, Influence of Magnesium on Grain Refinement and Ductility in a Dilute Al-Sc Alloy, *Acta Mater.*, 2001, **49**, p 3829–3838
27. Y. Peng, Z. Yin, B. Nie, and L. Zhong, Effect of Minor Sc and Zr on Superplasticity of Al-Mg-Mn Alloys, *Trans. Nonferr. Met. Soc. China*, 2007, **17**, p 744–750
28. R.R. Sawtell and G.L. Jensen, Mechanical Properties and Microstructures of Al-Mg-Sc Alloys, *Metall. Trans. A*, 1990, **21**, p 421–430
29. T.G. Nieh, L.M. Hsiung, J. Wadsworth, and R. Kaibyshev, High Strain Rate Superplasticity in a Continuously Recrystallized Al-6%Mg-0.3%Sc Alloy, *Acta Mater.*, 1998, **46**(8), p 2789–2800
30. Z. Horita, M. Furukawa, M. Nemoto, A.J. Barnes, and T.G. Langdon, Superplastic Forming at High Strain Rates After Severe Plastic Deformation, *Acta Mater.*, 2000, **48**(14), p 3633–3640
31. S. Komura, Z. Horita, M. Furukawa, M. Nemoto, and T.G. Langdon, An Evolution of the Flow Behavior During High Strain Rate Superplasticity in an Al-Mg-Sc Alloy, *Metall. Mater. Trans. A*, 2001, **32**, p 707–716
32. N. Balasubramanian and T.G. Langdon, An Analysis of Superplastic Flow After Processing by ECAP, *Mater. Sci. Eng. A*, 2005, **410**, p 476–479
33. J. Röyset, Scandium in Aluminium Alloys Overview: Physical Metallurgy, Properties and Applications, *Metall. Sci. Technol.*, 2007, **25**(2), p 11–21
34. F. Musin, R. Kaibyshev, Y. Motohashi, and G. Itoh, Superplastic Behavior and Microstructure Evolution in a Commercial Al-Mg-Sc Alloy Subjected to Intense Plastic Straining, *Metall. Mater. Trans. A*, 2004, **35**, p 2383–2392
35. D.A. Hughes, M.E. Kassner, M.G. Stout, and J.S. Vetrano, Metal Forming at the Center of Excellence for the Synthesis and Processing of Advanced Materials, *JOM*, 1998, **50**(6), p 16–21
36. J. Hedworth and M.J. Stowell, The Measurement of Strain-Rate Sensitivity in Superplastic Alloys, *J. Mater. Sci.*, 1971, **6**, p 1061–1069
37. T.R. McNelly, M.E. McMahon, and S.J. Hales, An EBSP Investigation of Alternate Microstructures for Superplasticity in Aluminium-Magnesium Alloys, *Scr. Mater.*, 1997, **36**(6), p 369–375
38. M.T. Pérez-Prado, G. Gonzáles-Doncel, O.A. Ruado, and T.R. McNelly, Texture Analysis of the Transition from Slip to Grain Boundary Sliding in a Discontinuously Recrystallized Superplastic Aluminium Alloy, *Acta Mater.*, 2001, **49**(12), p 2259–2268
39. T. Sakuma and K. Higashi, Summary in the Project "Towards Innovation in Superplasticity", *Mater. Trans. JIM*, 1999, **40**(8), p 702–715